Deep Mining 2024 – P Andrieux & D Cumming-Potvin (eds)

doi:10.36487/ACG_repo/2465_67

Seismic response during a mining stoppage

Daryl Rebuli [a,*]

[a] *Institute of Mine Seismology, Canada*

Abstract

Seismic monitoring after mine closures usually falls to the regional seismic monitoring system as the in-mine array is typically decommissioned during the early stage of the mine closure. This generally means only the larger seismic events are recorded and the location accuracy is usually enough to indicate that the event was on the mine. This paper examines two cases, from in-mine seismic arrays, where the mines stopped production for a significant period. The first case was for a period of more than a year and a half, in the seismically active region of the mine, while the second case was for approximately 50 days. In both cases the seismicity was found to diffuse in space as the duration of the stoppage increased. The time between successive events also noticeably increased the longer the stoppage continued. Seismicity induced by water ingress on closed mines have been studied by other authors over the years. For this study, the water ingress was controlled as the mines did not stop pumping. Therefore, the results found here are not associated with induced seismicity from flooding.

Keywords: *seismicity, mine closure, mine stoppage*

1 Introduction

In most cases, when mines close the installed seismic system is removed as part of the decommissioning process. This means that monitoring of any seismicity during and after the closure is restricted to any regional seismic monitoring arrays which may be present.

A few authors have reported work on seismicity after mine closure (for example Srinivasan et al. 2000; Goldbach 2009; Browitt & Walker 2019). In most cases the larger seismic events recorded by the regional systems were attributed to groundwater recharge. Ogasawara et al. (2002) also noted that rising water may have been a factor responsible for the observed increase in pore pressure in an old, flooded mine. These regional seismic networks don’t have the resolution or location accuracy to record the smaller events most likely occurring near the old mine.

This paper examines two cases, from in-mine seismic arrays, where the mine stopped for a significant period. The first was Beaconsfield mine in Australia, which was closed after the large seismic event of April 2006. Although mining started again in late 2006, in a region away from the seismically active region. Blasting, in the seismically active region, started again more than a year later in August 2007. The second case was for a mine in Canada which stopped production and development blasting for approximately 50 days during the first round of COVID-19 restrictions in Canada.

In this paper we look at two effects, one being the distance between successive events and the other the time between successive events. The thought is that the distance between events may indicate if the events are diffusing as the mining-induced stresses are allowed to relax, while the time between events indicates the relaxation of the disturbed stresses over time.

*Corresponding author. Email address: daryl.rebuli@imsi.org

One method to measure variation in a collection of data is to make use of the Coefficient of Variation (CV):

$$CV = \frac{\sigma}{\mu} \tag{1}$$

where:

σ = the standard deviation.

μ = mean of the collection.

This measures how much variation there is in the data. In this paper the variation in the distance and time between successive events is measured with the CV, using a sliding window of 20 events.

2 Beaconsfield mine

2.1 Context

On 25 April 2006 a ML2.3 seismic event resulted in one fatality, trapped two miners and caused significant damage (Pike 2006). The mine was closed while the incident was investigated. It was only late in 2007 that mining in the seismically active region of the mine started again.

The in-mine seismic array consisted of nine 14 Hz uniaxial geophones and one 14 Hz triaxial geophone. The layout is shown by blue tetrahedrons in Figure 1. The sensor coverage was localised, covering the deeper section of the mine at the time. In September 2007, the array was expanded to include two 4.5 Hz triaxial sensors, two 14 Hz triaxial sensors and two 14 Hz uniaxial sensors, shown in orange in Figure 1.

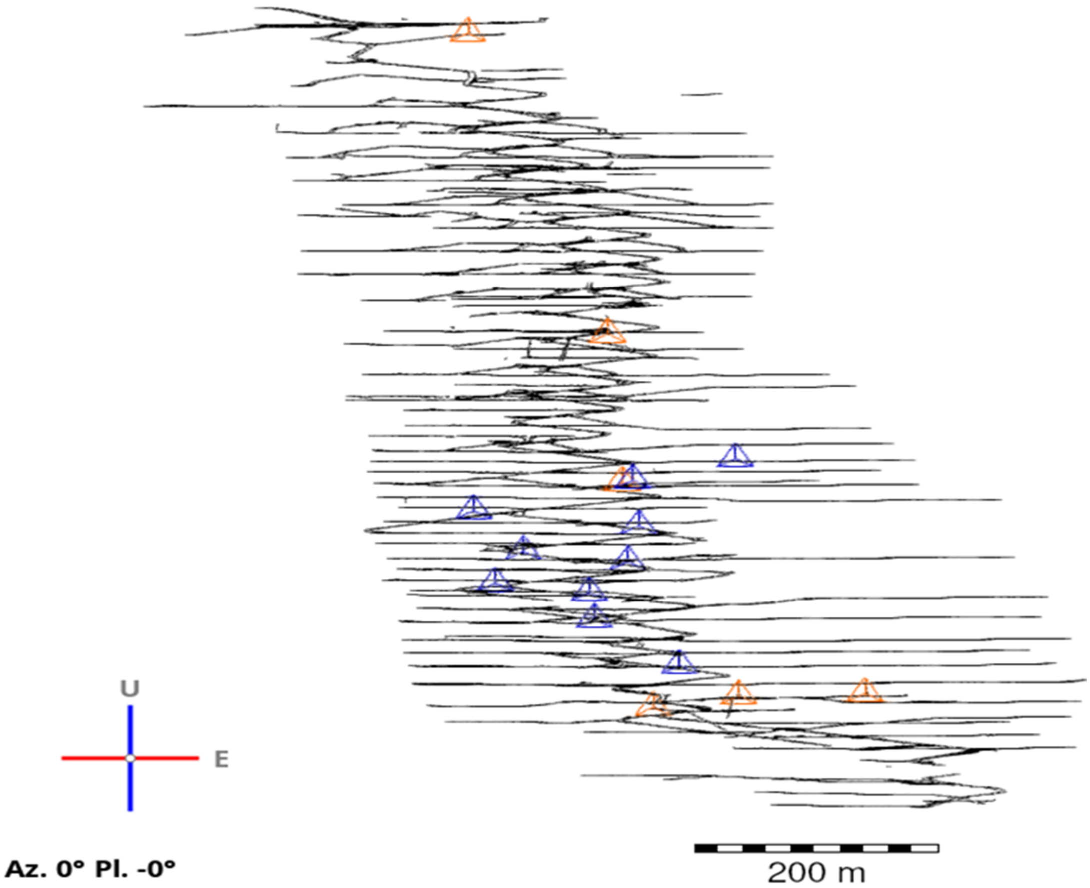

Figure 1 Section view showing the sensor layout for the seismic array at Beaconsfield mine. The sensors as of April 2006 are indicated as blue tetrahedrons, while the sensors added in September 2007 are shown as orange tetrahedron

2.2 Seismicity

Figure 2 shows the time history of the seismic activity for the period 2006 to mid-2008. This shows a significant decrease in the activity rate after the large event, with this only picking up again at the end of 2007.

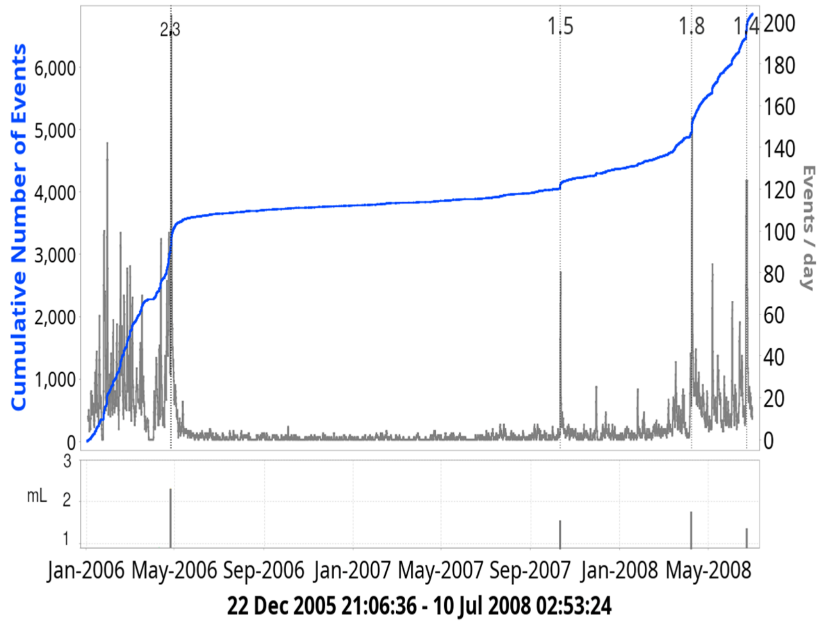

Figure 2 Time history of seismicity at Beaconsfield mine. The larger events are indicated on the plot

The events for this period mostly cluster in one section of the mine (Figure 3).

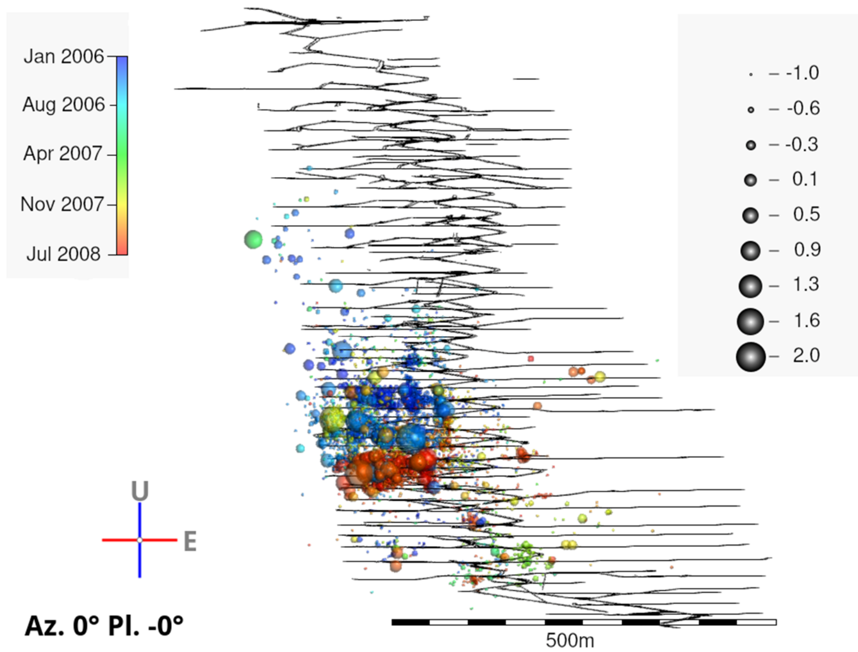

Figure 3 Section view showing the locations of seismicity at Beaconsfield mine for the period of interest

A plot of the size distribution for two periods, when mining was underway and for the period directly after the large event, is shown in Figure 4. The seismicity in the two active periods were very similar. Significantly fewer events were recorded during the stoppage.

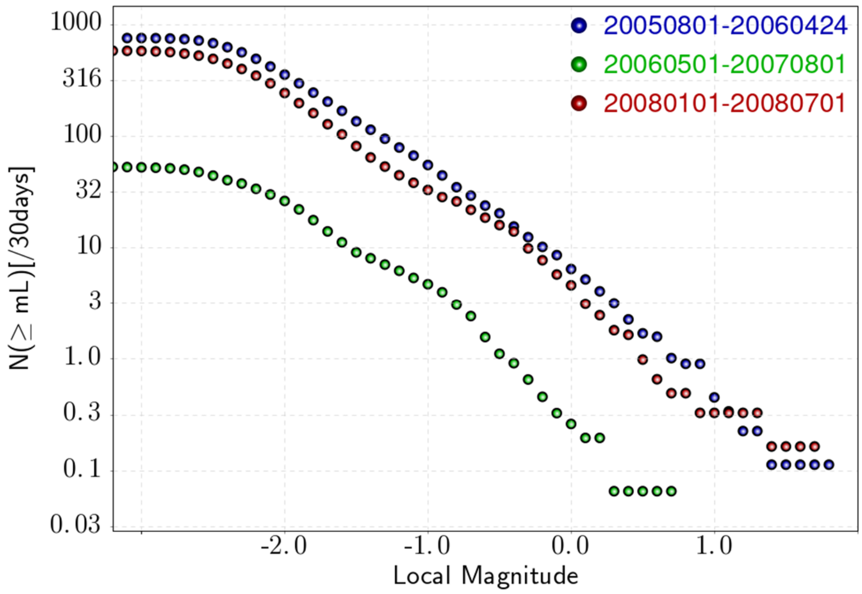

Figure 4 **Size distribution plot comparing before the large event (20050801-20060424), after the event while no mining was taking place in the seismically active region (20060501-20070801) and for a period when mining was underway again (20080101-20080701). The activity rates have been normalised to 30 days. The seismic behaviour during the two mining periods were very similar, while during the stoppage, the activity rate was significantly lower**

2.3 Response to large event

After the large event of April 2006, a flurry of events was recorded which decayed over time, following an exponential decay rate (Omori 1894; Utsu 1961) as shown in Figure 5. The events located in a few clusters around the active mining (Figure 6). These clusters were still close to each other and within the seismic array. Two ML1.1 events were recorded within 24 hours of the large event. No events larger than ML1.0 were recorded after this until after production started in the area again in late 2007.

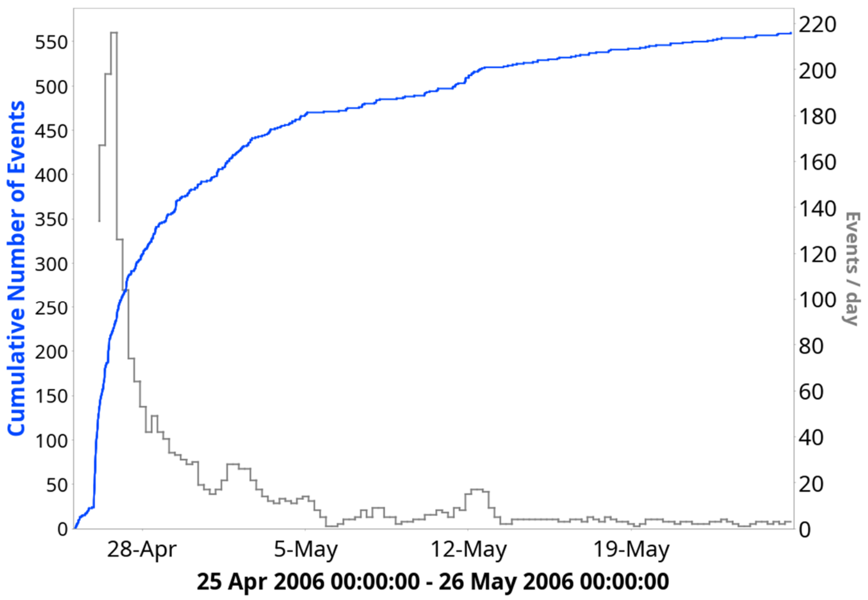

Figure 5 **Time history showing the seismic response during and after the large event on 25 April 2006**

The time history shows the decrease in the activity rate after the large event, but it is difficult to see in this plot how the seismicity changed while no mining was taking place.

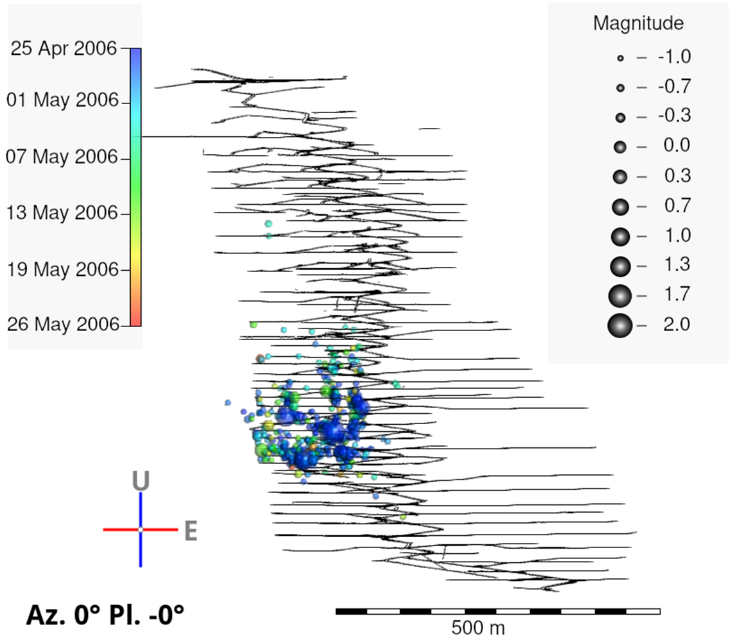

Figure 6 Section view showing the seismic response during and after the large event on 25 April 2006

2.4 Distance between successive events

The CV of distance between successive events before the large event of April 2006 shows some variation between 0.25 and 1.5 (Figure 7). After the large event the distance between successive events did increase, with the CV ranging between 0.5 and 2.5, until mining started in the region again. The increase in CV indicates the events were diffusing in space.

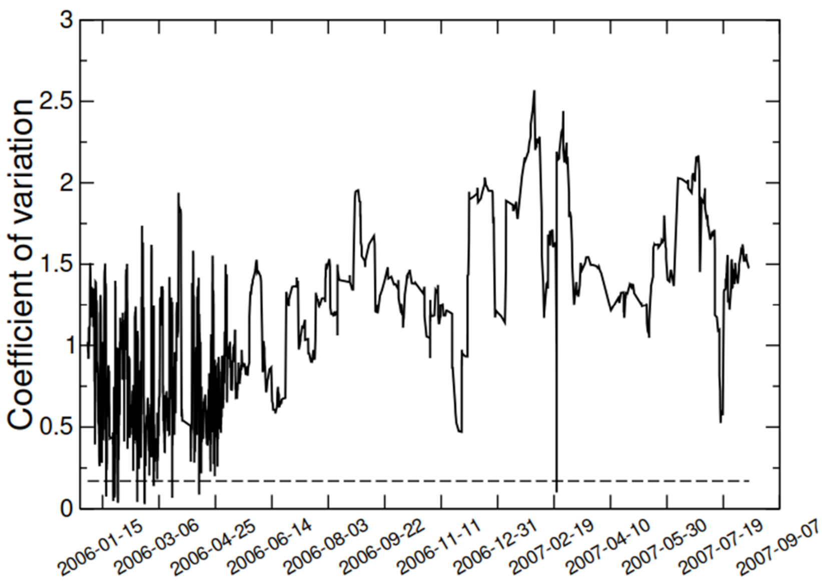

Figure 7 Plot of Coefficient of Variance for distance between successive events, based on a 20-event sliding window. The dashed line represents the location accuracy of the seismic array, which was estimated, from the seismic data, to be 16 m

The time between successive events remains low before the large event (Figure 8) but does increase quite significantly after this, until a small flurry is recorded around the 20 February 2007, when mining in an oredrive away from the seismically active region recommenced. The time between events increased quite quickly after this small flurry until mining activities in the seismically active region of the mine start on 23 August 2007. The increase in the time between successive events is expected, as originally reported by Omori (1894).

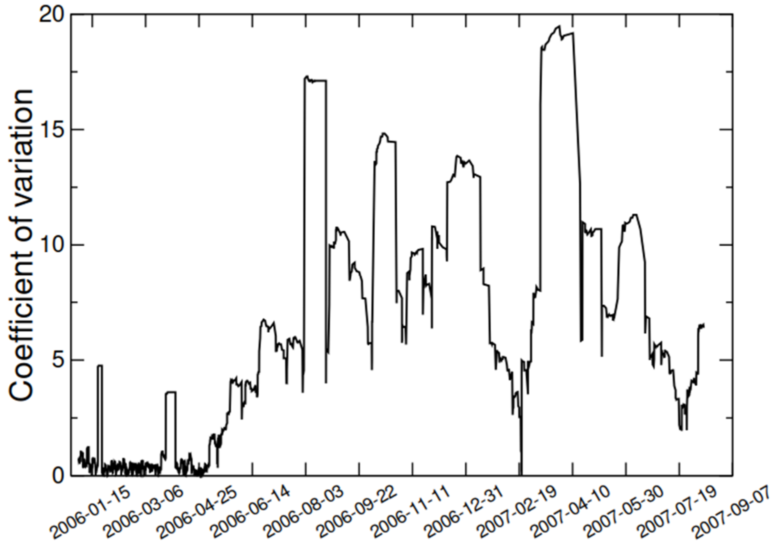

Figure 8 Plot of Coefficient of Variance for time between successive events, based on a 20-event sliding window

3 Mine B

3.1 Context

This Canadian mine has a much larger seismic system, consisting of 48 sensors (combination of uniaxial and triaxial geophones and accelerometers), covering a larger volume. The sensor array is shown in Figure 9.

Production and development blasts were halted for a period of 50 days (23 March to 12 May 2020) during the early part of the COVID-19 pandemic.

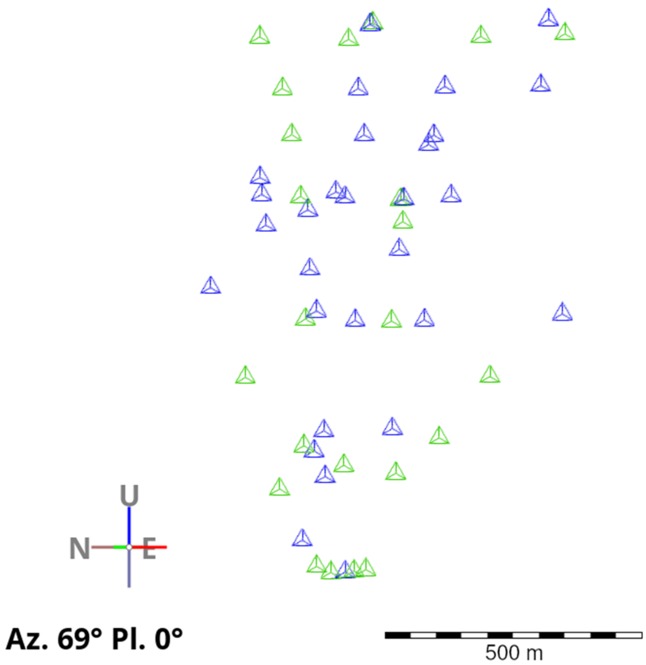

Figure 9 Section view showing the seismic sensors. The blue symbols are triaxial geophones and accelerometers, while the green symbols are uniaxial geophones and accelerometers

3.2 Seismicity

Mining was over multiple horizons over an approximate 1,000 m depth range, and the clusters of seismicity are shown in Figure 10. The events in this period locate around the active mining fronts.

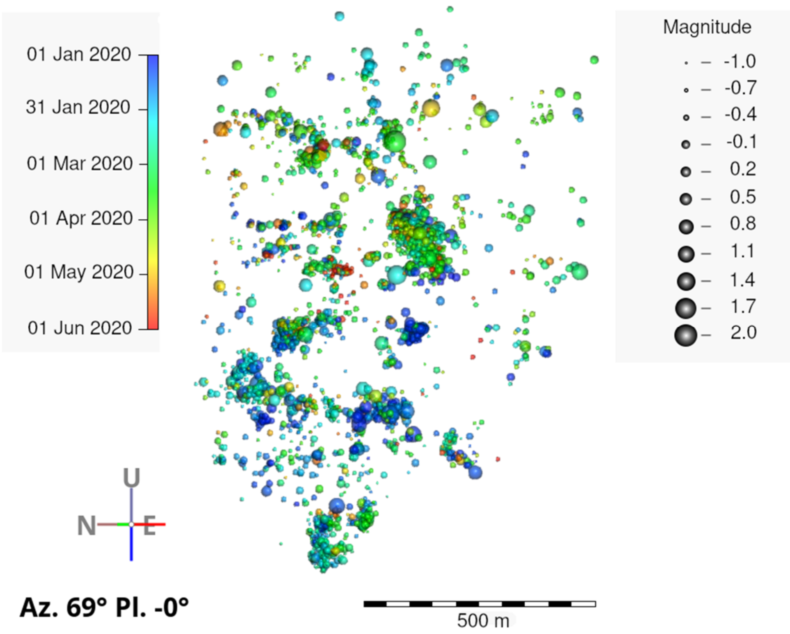

Figure 10 Section view showing the seismic events for the period 1 January to 1 June 2020. The events cluster around several active mining horizons

For the duration of the mining halt, the seismic system was operating, with no significant interruptions.

3.3 Response to blasting

The response to the last blasts before mining stopped is shown in Figures 11 and 12. On this day, three stopes were blasted of differing volumes, although on similar elevations.

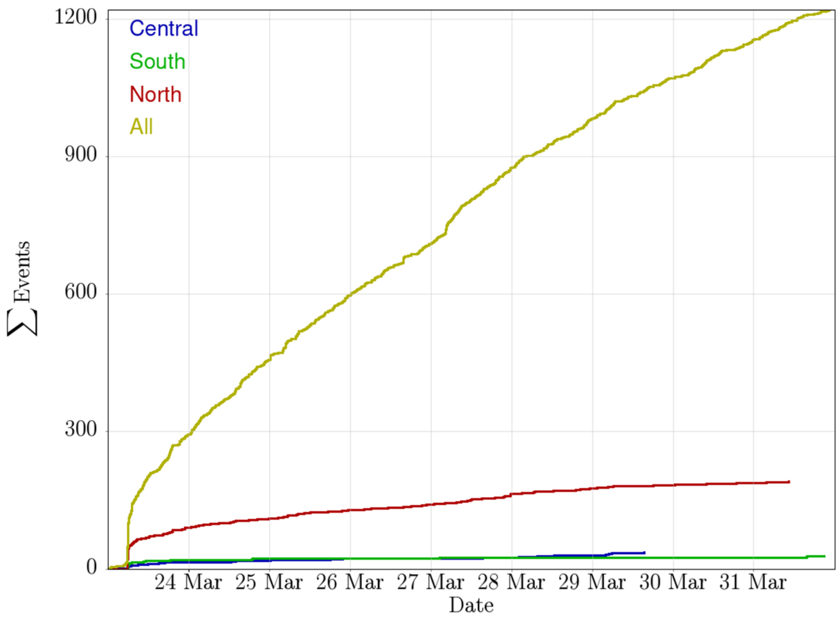

Figure 11 Time history of the seismicity after the production blasts on the 23 March 2020. All indicates the whole mine, while central, south and north are for the three regions around the production blasts on the 23 March 2020

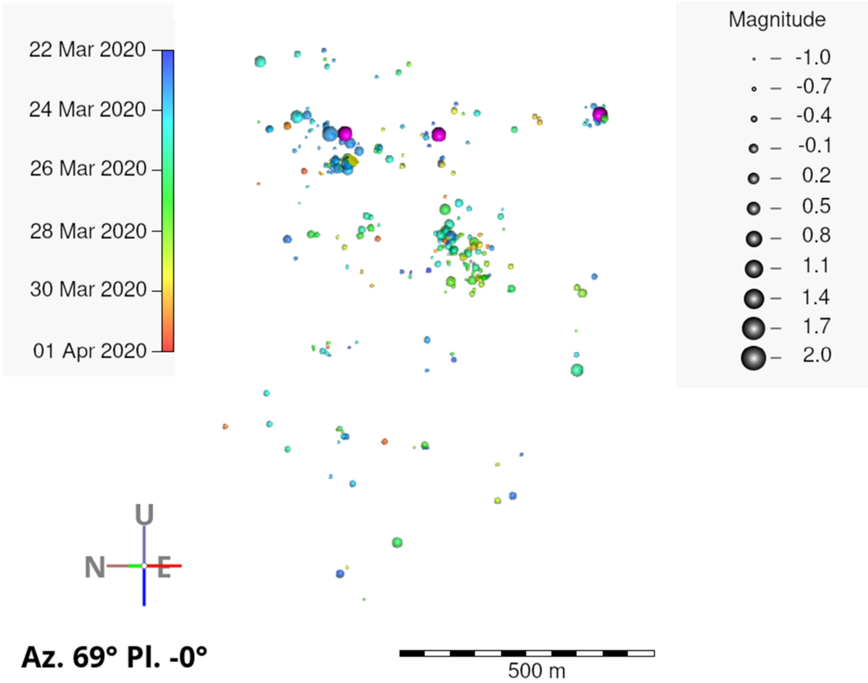

Figure 12 Section view showing the seismic response to the blasts on the 23 March 2020. The purple spheres indicate the stopes which were blasted on the 23, north, central and south from left to right

Figure 13 shows the time history for the events clustering around each of the blasts on the 23 March 2020. In terms of volume mined, the South stope was almost 50% larger than the North stope. The North stope was about 50% larger than the Central stope. Figure 14 shows the size distribution for the seismic response of the three stopes.

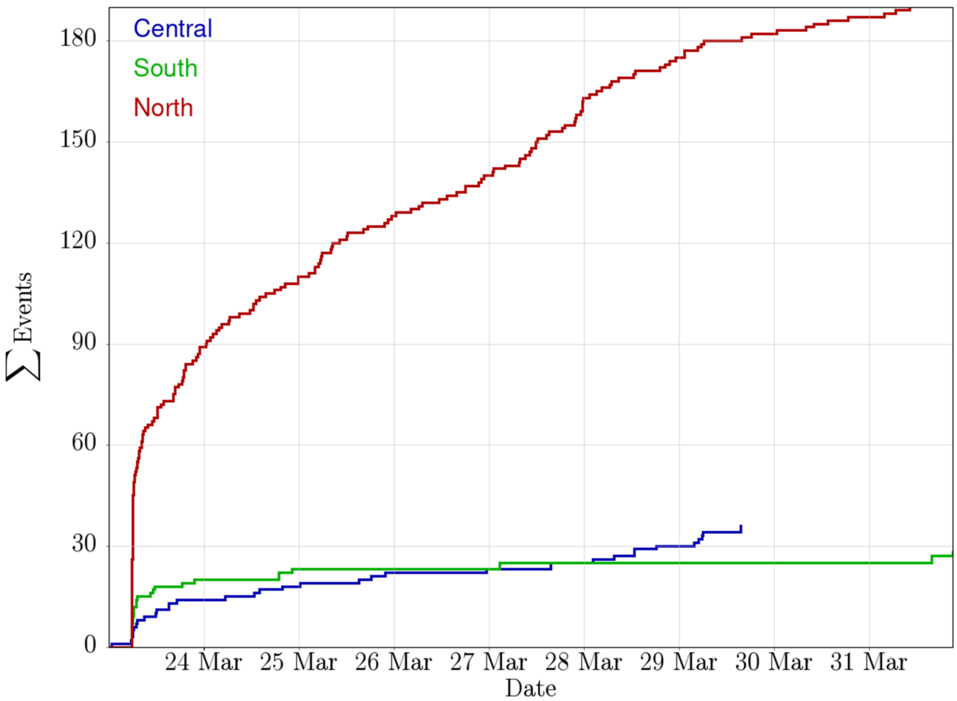

Figure 13 Time history of the seismicity after the production blasts on the 23 March 2020. In this plot, only the events around each of the stopes blasted are shown

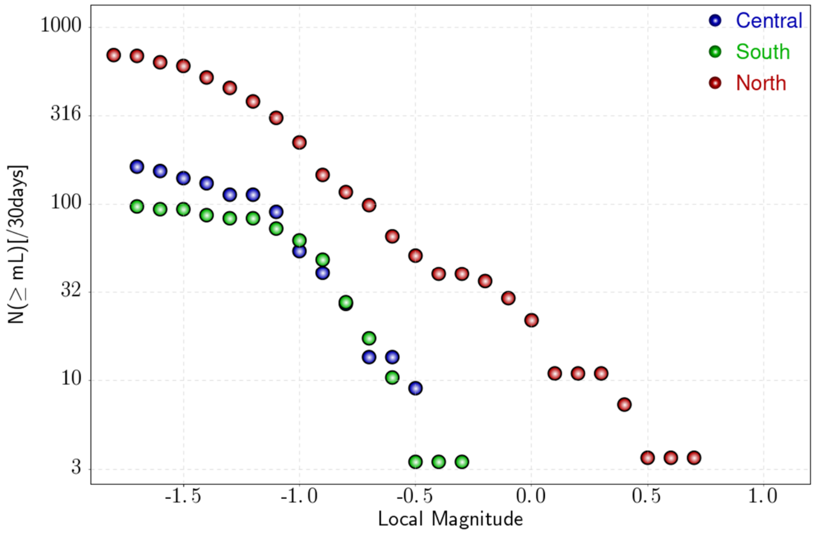

Figure 14 Size distribution of the seismicity after the production blasts on the 23 March 2020, separated spatially around each blast

The Central and South stope had similar responses, despite the difference in size of the blasts. The North stope had a much stronger seismic response compared with the other two. In terms of mining the South stope is at the edge of the mining, with little historic mining nearby. The extraction ratio is less than 20% in this region. The Central stope has historically mined stopes above and below with an extraction ratio close to 60%, while the North stope somewhat in between in terms of historic mining, with an extraction ratio of around 40%.

3.4 Distance between successive events

Figure 15 shows the CV of distance between successive events for March to June 2020 for the whole mine. No significant variation in the distance between successive events is observed. This may be because seismicity is recorded over a large volume of the mine with multiple seismogenic regions.

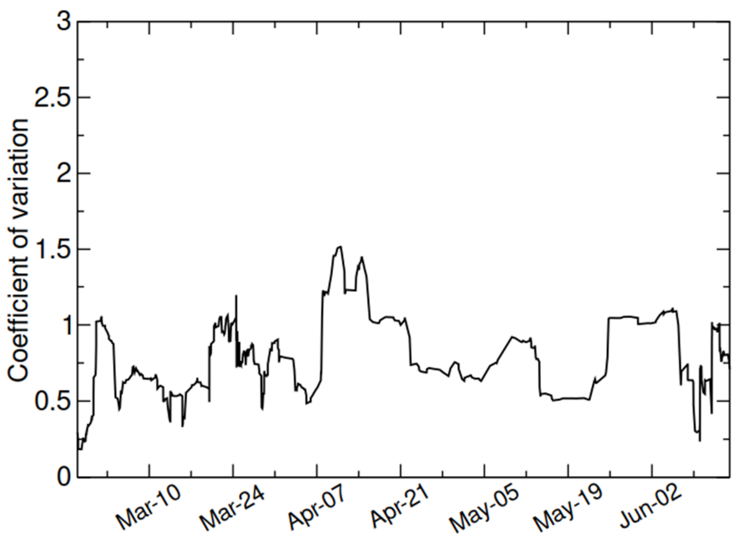

Figure 15 Coefficient of variation for distance between successive events at the mine for the period 1 March to 22 June 2020. A 20-event sliding window was used

For this reason, two smaller regions were selected as shown in Figure 16. The North cluster, used above was chosen because of the significant number of events recorded. The Central and South clusters were not used because of the much smaller activity rates in these regions. A fourth cluster, with a significant number of events for the period considered, was selected. The limitation here is that the maximum distance between events is then limited by the size of the sub-volume or cluster, and it is possible that events outside the volume may be because of stress redistribution from the events inside the volume.

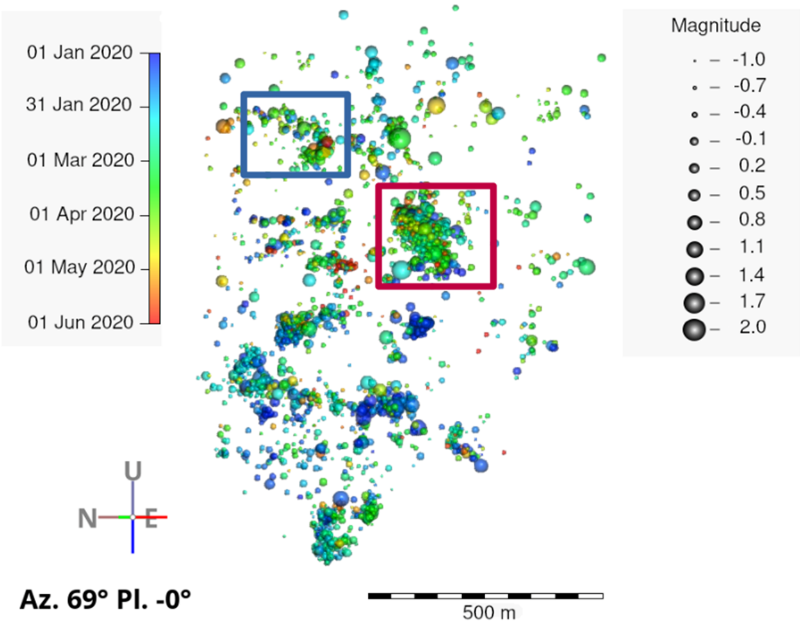

Figure 16 Section view showing the seismic events for the period 1 January to 1 June 2020. Two sub-regions (region 1 in blue and region 2 in red) were selected for further analysis

The location accuracy of events in each region are shown by the purple surfaces in Figure 17. These are shown as dashed lines in Figure 18, which shows the variation in the distance between successive events for the two regions. This does show some diffusion of seismicity in region 1 but is more obvious in region 2.

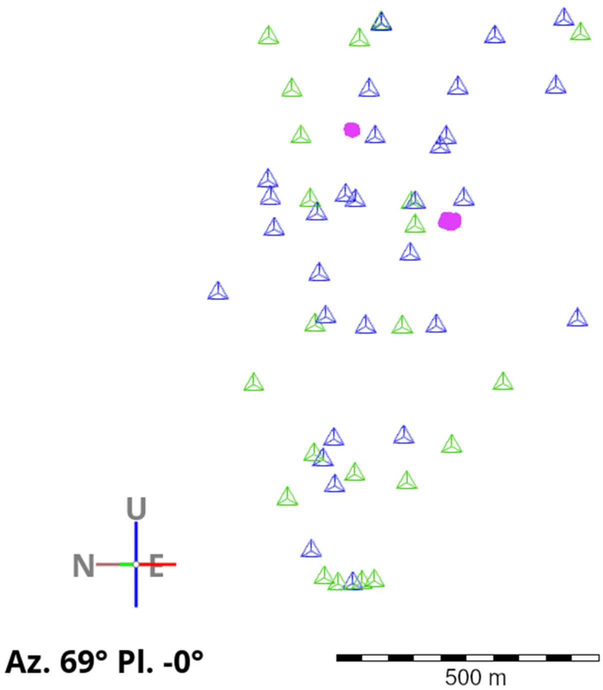

Figure 17 Seismic event location accuracy for the two regions of interest. The purple blobs were obtained from a Monte Carlo simulation of the location accuracy of events in each region. These were 25 and 30 m from left to right

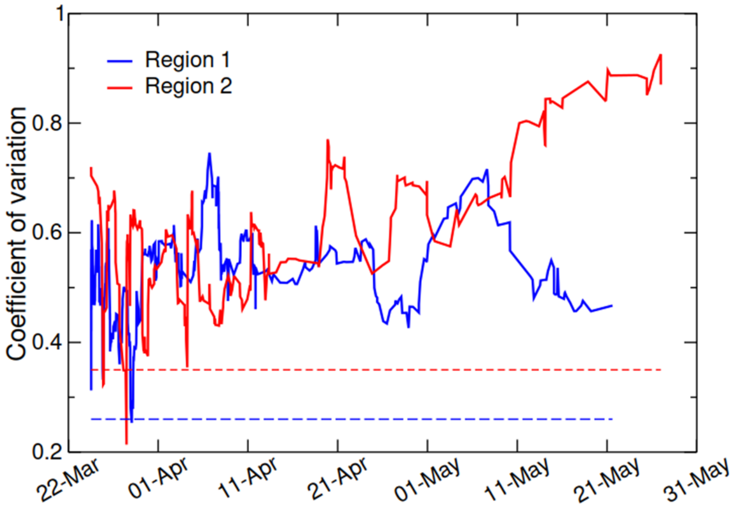

Figure 18 Coefficient of variation for distance between successive events for the two regions. A 20-event sliding window was used. The dashed lines represent the location accuracy in each of the regions

3.5 Time between successive events

The variation time between successive events for the same time period is shown in Figure 19. After the last blast on 23 March 2020, the time between events does increase while no production or development was taking place.

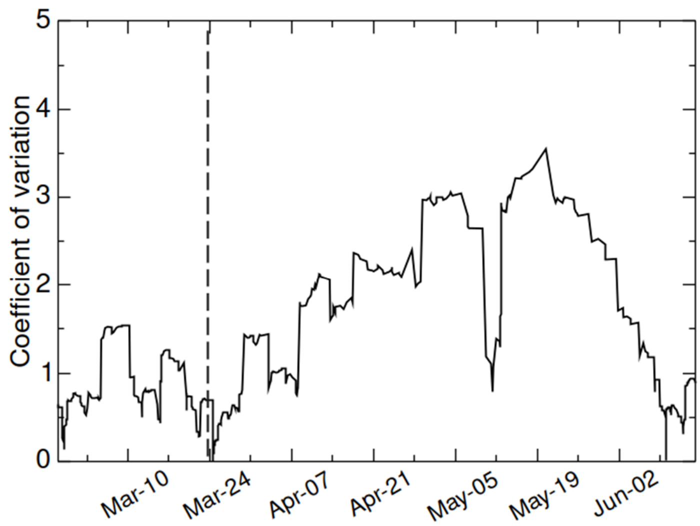

Figure 19 Coefficient of variation for time between successive events at the mine for the period 1 March to 22 June 2020. A 20-event sliding window was used. The vertical dashed line indicates the time of the last blast before the stoppage

4 Comparison and discussion

The two cases discussed above have two major differences, one being the volume of the mine, which was seismically active, and the other, the duration of the stoppage.

In terms of the volume of the seismically active region of the mine, the seismicity recorded at Beaconsfield mine for the period of interest was mostly constrained to near where the large event occurred. Some diffusion of the seismicity was observed during the stoppage. For mine B, the seismically active volume was significantly larger, with seismic responses to mining occurring on multiple mining horizons. While mining was stopped at mine B, the distance between successive events did not show much variation compared to periods when mining was taking place. This is mostly due to large volume, encompassing multiple seismogenic zones. Looking at smaller volumes within the mine, an increase in variation is observed especially in region 2, suggesting diffusion of seismicity during the stoppage, even over a short time period. Stress equilibrium may not have been reached within the 50 days.

In terms of duration of stoppage, the stoppage at Beaconsfield mine was significantly longer compared with mine B. However, for both mines, the variation in time between successive events did increase noticeably during the stoppage periods.

In mine B, a ML1.3 event was recorded mid-way through the stoppage. This indicates that the stress redistribution from the residual seismicity may be enough to trigger/induce larger failures. This study was not able to determine how long this may persist, as in the one case, a stoppage of over a year did not result in any significantly large seismic events, while, in the second case, a stoppage of 50 days did. The mining geometry and local stress conditions would play a large role here, along with water ingress in the case of a permanent mine closure.

5 Conclusion

This paper examines two cases, from in-mine seismic arrays, where the mine stopped for a significant period.

In the first case, where seismicity was localised, the seismicity did tend to diffuse in space as the duration of the stoppage increased. For the mine with a larger seismically active volume, smaller volumes did show a similar trend of diffusion. In both cases, the time between successive events noticeably increased the longer the stoppage continued. In the second case, it is likely that the 50 days was not long enough for the local stress redistribution to reach equilibrium.

In both cases water ingress was managed during the mine stoppages, and so groundwater recharge were not the cause of seismicity during the stoppage periods. Although the effect of water ingress could not be studied here, other papers indicate this may be a concern for mine closures.

Acknowledgement

Thank you to the mine in Canada for allowing these results to be published.

References

Browitt, C & Walker, A 2019, 'Induced seismicity in the UK is commonplace!', *2019 SECED Conference: Earthquake Risk and Engineering Towards a Resilient World*, Society for Earthquake and Civil Engineering Dynamics, Greenwich.

Goldbach, O 2009, 'Seismic risks posed by mine flooding', *Hard Rock Safe Safety Conference 2009: A Sense of Safety Urgency*, The Southern African Institute of Mining and Metallurgy, Johannesburg.

Ogasawara, H, Kuwabara, Y, Miwa, T, Fujimori, K, Hirano, N & Koizumi, M 2002, 'Post-seismic effects of an M 7.2 earthquake and microseismicity in an abandoned, flooded, deep mine', *Pure and Applied Geophysics*, vol. 159, pp. 63–90.

Omori, F 1894, 'On the aftershocks of earthquakes', *Journal of the College of Science*, Imperial University of Tokyo, vol. 7, pp. 111–200.

Pike, P 2006, 'Media management – Beaconsfield mine collapse', *Australian Journal of Emergency Management*, vol. 21, no. 3.

Srinivasan, C, Benady, S & Sivakumar, C 2000, 'Fluid induced seismicity in the Kolar mining region', *Workshop on Dam Safety*, Central Board of Irrigation and Power, Thiruvananthapuram.

Utsu, T 1961, 'A statistical study of the occurrence of aftershocks', *Geophysical Magazine*, vol. 30, pp. 521–605.